

Derivation of the bacterial run-and-tumble kinetic equation from a model with biochemical pathway

Benoît Perthame*

Min Tang[†]

Nicolas Vauchelet*

March 15, 2016

Abstract

Kinetic-transport equations are, by now, standard models to describe the dynamics of populations of bacteria moving by run-and-tumble. Experimental observations show that bacteria increase their run duration when encountering an increasing gradient of chemotactic molecules. This led to a first class of models which heuristically include tumbling frequencies depending on the path-wise gradient of chemotactic signal.

More recently, the biochemical pathways regulating the flagellar motors were uncovered. This knowledge gave rise to a second class of kinetic-transport equations, that takes into account an intra-cellular molecular content and which relates the tumbling frequency to this information. It turns out that the tumbling frequency depends on the chemotactic signal, and not on its gradient.

For these two classes of models, macroscopic equations of Keller-Segel type, have been derived using diffusion or hyperbolic rescaling. We complete this program by showing how the first class of equations can be derived from the second class with molecular content after appropriate rescaling. The main difficulty is to explain why the path-wise gradient of chemotactic signal can arise in this asymptotic process.

Randomness of receptor methylation events can be included, and our approach can be used to compute the tumbling frequency in presence of such a noise.

Key words: kinetic-transport equations; chemotaxis; asymptotic analysis; run and tumble; biochemical pathway;

Mathematics Subject Classification (2010): 35B25; 82C40; 92C17

1 Introduction

Two classes of kinetic-transport equations have been proposed to describe, at the cell scale, the movement of bacteria by ‘run and tumble’ in a given external effective signal $M(x, t)$, usually related to the extra-cellular chemo-attractant concentration S by a relation of the type $M = m_0 + \ln(S)$.

*Sorbonne Université, UPMC Univ Paris 06, Laboratoire Jacques-Louis Lions UMR CNRS 7598, Inria, F75005 Paris, France. This author is partially supported by ANR Kibord-ANR-13-BS01- 0004 funded by the French Ministry of Research

[†]Institute of natural sciences and department of mathematics, Shanghai Jiao Tong University, Shanghai, 200240, China. This author is partially supported by NSF of Shanghai under grant 12ZR1445400, NSFC 11301336 and 91330203, and Shanghai Pujiang Program 13PJ140700.

The simplest class is for the probability $\bar{p}(\mathbf{x}, \mathbf{v}, t)$ to find a bacteria at location $\mathbf{x} \in \mathbb{R}^d$ and with velocity $\mathbf{v} \in V$ (a smooth bounded subset of \mathbb{R}^d , one can choose the unit ball to fix idea). The evolution of this probability is given by a Boltzmann type equation

$$\partial_t \bar{p} + \mathbf{v} \cdot \nabla_{\mathbf{x}} \bar{p} = \mathcal{T}[D_t M](\bar{p}), \quad \mathbf{x} \in \mathbb{R}^d, \mathbf{v} \in V, t \geq 0, \quad (1)$$

with the path-wise gradient of M defined as

$$D_t M(x, \mathbf{v}, t) = \partial_t M(x, \mathbf{v}, t) + \mathbf{v} \cdot \nabla_{\mathbf{x}} M(x, \mathbf{v}, t) \quad (2)$$

and T a tumbling kernel which typically takes the form

$$\mathcal{T}[D_t M](\bar{p}) = \int_V [T(D_t M(\mathbf{x}, \mathbf{v}', t), \mathbf{v}, \mathbf{v}') \bar{p}(\mathbf{x}, \mathbf{v}', t) - T(D_t M(\mathbf{x}, \mathbf{v}, t), \mathbf{v}', \mathbf{v}) \bar{p}(\mathbf{x}, \mathbf{v}, t)] d\mathbf{v}'. \quad (3)$$

The left hand side of equation (1) models the run phase, whereas the right hand side describes the velocity jump process during the tumbling. Such equations, with \mathcal{T} depending on M or $D_t M$, were used intensively to model bacterial chemotaxis, possibly with M connected to the cell density, as a result of chemoattractant release by bacteria. They were first introduced in [18] and the Keller-Segel drift-diffusion system was subsequently derived [19] in the diffusion limit; surprisingly, with a kernel T depending on M and not on its gradient, and in opposition to the Keller-Segel system which solutions blow-up for large mass, it was proved that the solutions exist globally [5, 12]. However, experiments show that bacteria as *E.coli* extend their runs when feeling an increasing concentration of chemoattractant and this led to study tumbling kernels T that depend on $D_t M$, see [8, 6]. The nonlinear theory is then more difficult (see [4] and the references therein) and blow-up can occur in finite time [2]. These models with T depending on $D_t M$ are able to explain the experimental observation of traveling pulses of bacteria, which cannot be done when T only depends on M itself, see [23, 24]. Also, departing from this kinetic-transport equation, it is possible to rescale it and study the diffusion and hyperbolic limit as in [8, 6, 23, 24, 12, 11]. When T undergoes stiff dependency on $D_t M$, the hyperbolic limit is singular and the analysis is particularly delicate [13].

Actually, the response of bacteria to signal changes is orchestrated by a sophisticated chemotactic signal transduction pathway, which involves a rapid response of the cell to the external signal change called 'excitation', and a slow 'adaptation' which allows the cell to subtract out the background signal. In order to incorporate this intracellular chemo-sensory system, more elaborated kinetic models have been proposed. In [8, 9], a cell-based model which incorporates a linear cartoon description of the excitation and adaptation response of a cell has been introduced. The signal transduction pathway has been studied in e.g. [10, 20]. We refer to [20, 31] where the case of bacteria *E. coli* has been extensively detailed, other bacteria using similar strategies to move are encountered also in [22, 21]. In the simplest description of the biochemical pathways, a single additional variable $m \geq 0$, which represents the intracellular methylation level, is used. The intracellular adaptation dynamics is generally modeled by an ODE

$$\frac{dm}{dt} = f(m, M(x, t)),$$

where f describes the chemical reaction. We recall that M is the given external effective signal; it usually has a logarithmic dependency with the chemo-attractant concentration as it has been recently experimentally evidenced for *E. coli* in [15]. Then, the kinetic-transport equation governs the dynamic

of the probability density function $p(\mathbf{x}, \mathbf{v}, m, t)$ of bacteria at time t , position $\mathbf{x} \in \mathbb{R}^d$, moving at velocity $\mathbf{v} \in V$, where V is a bounded domain of \mathbb{R}^d , and methylation level $m > 0$. It reads

$$\begin{cases} \partial_t p + \mathbf{v} \cdot \nabla_{\mathbf{x}} p + \partial_m [f(m, M)p] = \mathcal{Q}[m, M](p), \\ p(\mathbf{x}, \mathbf{v}, m = 0, t) = 0. \end{cases} \quad (4)$$

We assume that the reaction rate $f(\cdot)$ verifies $f(m = 0, M) > 0$, which allows us to pose the boundary condition at $m = 0$. Here the \mathbf{x} -divergence term describes the change of probability due to the bacteria ‘run’, the m -derivative models the evolution of the methylation level. The tumbling term $\mathcal{Q}[m, M](p)$ describes the velocity jump process, it is given by

$$\mathcal{Q}[m, M](p) = \int_V [\lambda(m, M, \mathbf{v}, \mathbf{v}')p(t, \mathbf{x}, \mathbf{v}', m) - \lambda(m, M, \mathbf{v}', \mathbf{v})p(t, \mathbf{x}, \mathbf{v}, m)] d\mathbf{v}', \quad (5)$$

where $\lambda(m, M, \mathbf{v}, \mathbf{v}')$ denotes the methylation dependent tumbling frequency from \mathbf{v}' to \mathbf{v} , in other words the response of the cell depending on its environment and internal state. We borrow this formalism from [14, 25] even though this type of models, involving more general signal transduction, can be traced back to [8, 9, 6, 30]. The authors in [8, 9, 6, 30, 25, 31] developed the asymptotic theory which, departing from the kinetic level of description, allows to recover, in the diffusion and in the hyperbolic limits, macroscopic equations where the variables are only (\mathbf{x}, t) as the Keller-Segel system which governs the dynamics of the density of cells.

In the program of establishing the relations between these pieces of the model hierarchy for bacterial population motion, a derivation is missing: how are related these two classes of kinetic models (1)–(3) and (4)–(5)?

In this paper, we focus on the mathematical link between these classes of kinetic models. To this aim, we assume a fast adaptation and stiff response of the internal states, the methylation level is then at equilibrium with the external signal represented by M , and the equation (1) can be derived from (4). In particular, we aim at computing the bulk tumbling kernel $T(D_t M, \mathbf{v}, \mathbf{v}')$ from the methylation dependent kernel $\lambda(m, M, \mathbf{v}, \mathbf{v}')$, a statement we give in the next section. Two difficulties arise here: one is to infer the proper rescaling in the kinetic equations, the second is to carry-out the mathematical analysis for singular limits. We also show the robustness of our approach by including a structural change in the equation. The proof of the formula for T is given in sections 3 and 4; we show that a direct use of the variable m is not enough to produce the formula and that a new variable is needed, which zooms on the intra- and extra-cellular methylation equilibrium. In section 5, we relate our notations to a more physically based description of the same model where the cell receptors activity is used in the model parameters. This model has been used as a comprehensive model based on details biochemistry of *E. coli* chemotaxis. In this physical framework, numerical comparisons between the two kinetic models are considered in section 6. We conclude by a discussion on the validity of our assumption.

To keep simplicity, we assume that the external signal function $M(\mathbf{x}, t)$ is given and smooth. Therefore questions of existence and blow-up are not considered here.

2 Fast adaptation, stiff response

Assumptions. For our mathematical derivation, we introduce a small parameter ϵ which acts both as a fast time scale for external signal transduction and as a stiffness parameter for the response in terms of tumbling rate. More precisely, the external signal transduction is assumed to fastly relaxes towards equilibrium, which is modeled by the intracellular adaptation dynamics

$$\frac{dm}{dt} = \frac{1}{\epsilon} f(m - M(\mathbf{x}, t)).$$

Such dependancy of the reaction rate f on the difference $m - M$ is in accordance with the physical models that we recall in Section 5. We model the stiff response of the internal variable by assuming that the tumbling frequency is a fast varying function: $\lambda(m, M, \mathbf{v}, \mathbf{v}') = \Lambda\left(\frac{m-M}{\epsilon}, \mathbf{v}, \mathbf{v}'\right)$. Therefore, equation (4)–(5) rescale as

$$\begin{cases} \partial_t p_\epsilon + \mathbf{v} \cdot \nabla_{\mathbf{x}} p_\epsilon + \frac{1}{\epsilon} \partial_m (f(m - M) p_\epsilon) = \mathcal{Q}_\epsilon[m, M](p_\epsilon), \\ p_\epsilon(\mathbf{x}, \mathbf{v}, m = 0, t) = 0, \end{cases} \quad (6)$$

with the tumbling kernel

$$\mathcal{Q}_\epsilon[m, M](p_\epsilon) = \int_V \left[\Lambda\left(\frac{m - M}{\epsilon}, \mathbf{v}, \mathbf{v}'\right) p_\epsilon(\mathbf{x}, \mathbf{v}', m, t) - \Lambda\left(\frac{m - M}{\epsilon}, \mathbf{v}', \mathbf{v}\right) p_\epsilon(\mathbf{x}, \mathbf{v}, m, t) \right] d\mathbf{v}'. \quad (7)$$

We complete this equation with an initial data $p^{\text{ini}} \geq 0$ which satisfies

$$\iiint_{\mathbb{R}^d \times V \times \mathbb{R}} (1 + m^2) p^{\text{ini}}(\mathbf{x}, \mathbf{v}, m) d\mathbf{x} d\mathbf{v} dm < \infty, \quad (8)$$

$$\bar{p}^{\text{ini}} := \int_{\mathbb{R}} p^{\text{ini}} dm \in L^\infty(\mathbb{R}^d \times V). \quad (9)$$

Also, we are going to use several assumptions for the functions M , f and Λ . We assume they are as smooth as necessary and that for some constants m_\pm , g_\pm , λ_\pm ,

$$0 < m_- \leq M(\mathbf{x}, t) \leq m_+, \quad M \in C_b^1(\mathbb{R}^d \times [0, \infty)), \quad (10)$$

$$f(y) = -yG(y), \quad \text{with } G \in C_b^1(\mathbb{R}), \quad 0 < g_- \leq G(y) \leq g_+, \quad (11)$$

$$\partial_y \Lambda(y, \mathbf{v}, \mathbf{v}') < 0, \quad 0 < \lambda_- \leq \Lambda(y, \mathbf{v}, \mathbf{v}') \leq \lambda_+. \quad (12)$$

Various scalings have been proposed for kinetic equation and the closest, but still different seems to be the high field limit [1]. In [17], still other scalings or limits are studied.

The main result. With these assumptions, we are going to show that as ϵ vanishes, we recover the simpler model (1)–(3) as a limit of (6).

Theorem 2.1 (Derivation of the kinetic equation) *Let V be a bounded domain of \mathbb{R}^d . We make the assumptions (8)–(9) on the initial data, and (10)–(12) on the coefficients. Let p_ϵ be the solution to (6). Then, for all $T > 0$, \bar{p}_ϵ is bounded in $L^\infty([0, T] \times \mathbb{R}^d \times V)$ and*

$$\bar{p}_\epsilon := \int_{\mathbb{R}} p_\epsilon dm \xrightarrow[\epsilon \rightarrow 0]{} \bar{p}_0 \quad \text{in } L^\infty([0, T] \times \mathbb{R}^d \times V)\text{-weak-}\star$$

and \bar{p}_0 satisfies equation (1)–(3) with

$$T(u, \mathbf{v}, \mathbf{v}') = \Lambda\left(-\frac{u}{G(0)}, \mathbf{v}, \mathbf{v}'\right).$$

Furthermore, we have $\bar{p}_0 := \int_{\mathbb{R}} p_0 \, dm$ with p_0 the weak limit (in measures, see (15)) of p_ϵ which is given by

$$p_0(\mathbf{x}, \mathbf{v}, m, t) = \bar{p}_0(\mathbf{x}, \mathbf{v}, t) \delta(m = M(\mathbf{x}, t)).$$

Before we prove this theorem in the next sections, we show robustness of the limiting procedure.

Structural stability. To sustain the robustness of this limiting procedure, we consider a structural change in the model by adding a diffusion term in m . The model is as follows:

$$\partial_t p_\epsilon + \mathbf{v} \cdot \nabla_{\mathbf{x}} p_\epsilon + \frac{1}{\epsilon} \partial_m \left(f(m - M) p_\epsilon \right) - \epsilon \sigma \partial_{mm}^2 p_\epsilon = \mathcal{Q}_\epsilon[m, M](p_\epsilon), \quad (13)$$

with the no-flux boundary condition that now reads

$$f(-M) p_\epsilon(\mathbf{x}, \mathbf{v}, m, t) - \epsilon^2 \sigma \partial_m p_\epsilon(\mathbf{x}, \mathbf{v}, m, t) = 0, \quad \text{at } m = 0. \quad (14)$$

This additional term might also be interpreted as a simplified representation of internal noise resulting from random methylation and demethylation events on the thousands of receptors in *E. coli*, [7]. Again the particular scaling in ϵ is chosen to recover a distinguished limit

Theorem 2.2 (Limit with noise) *With the assumptions and notations of Theorem 2.1, the same conclusions hold for the solution p_ϵ of (13), with the same expression for p_0 and*

$$T_\sigma(u, \mathbf{v}, \mathbf{v}') = \sqrt{\frac{G(0)}{2\pi\sigma}} \int_{\mathbb{R}} \Lambda(y, \mathbf{v}, \mathbf{v}') e^{-\frac{G(0)}{2\sigma} \left(y + \frac{u}{G(0)}\right)^2} \, dy.$$

As a consequence, as σ vanishes, we recover the tumbling kernel T of Theorem 2.1 as a limit of T_σ .

A priori bounds and principle of the proof. Before we explain the derivation of the formula stated in these theorems, let us make some observations which explain the difficulty. Because we assume that $M(x, t)$ is given, we handle a linear equation for which existence and uniqueness of weak solutions is well established. The nonlinear case, when the chemoattractant concentration giving rise to M is coupled to p^ϵ , can also be treated, see [3, 17]. In particular we will make use of the uniform estimates (see Section 4)

$$\iiint_{\mathbb{R}^d \times V \times \mathbb{R}} p_\epsilon(\mathbf{x}, \mathbf{v}, m, t) \, d\mathbf{x} \, d\mathbf{v} \, dm = \iiint_{\mathbb{R}^d \times V \times \mathbb{R}} p^{\text{ini}}(\mathbf{x}, \mathbf{v}, m) \, d\mathbf{x} \, d\mathbf{v} \, dm, \quad \forall t \geq 0, \quad (15)$$

$$\bar{p}_\epsilon(\mathbf{x}, \mathbf{v}, t) \leq \|\bar{p}^{\text{ini}}(\mathbf{x}, \mathbf{v})\|_\infty e^{Ct}, \quad \forall t \geq 0, \quad (16)$$

where C is a nonnegative constant. From these bounds, we conclude that we can extract subsequences (but to simplify the notations we ignore this subsequence) which converge as mentioned in the theorems.

Passing to the limit in the equation on p_ϵ (with or without noise) gives us

$$\partial_m \left(f(m - M) p_0 \right) = 0.$$

This tells us that $f(m - M) p_0 = 0$ (it is constant and p_0 is integrable). Because, with assumption (11), $f(m - M)$ vanishes only for $m - M = 0$, we conclude that p_0 is a Dirac mass at $m = M$, hence the expression of p_0 in Theorems 2.1 and 2.2.

However this information is not enough to pass to limit in the equation on \bar{p}_ϵ obtained integrating in m equation (6) or (13), that is

$$\partial_t \bar{p}_\epsilon + \mathbf{v} \cdot \nabla_{\mathbf{x}} \bar{p}_\epsilon = \int_{\mathbb{R}^+} \mathcal{Q}_\epsilon[m, M](p_\epsilon) dm.$$

Indeed, in the right hand side, the product $\Lambda\left(\frac{m-M}{\epsilon}, \mathbf{v}, \mathbf{v}'\right) p_\epsilon(\mathbf{x}, \mathbf{v}', m, t)$ is, in the limit, a discontinuity multiplied by a Dirac mass. For this reason, we have to rescale in m in order to evaluate this limit, which we do in the next section.

3 The change of variable

To get a more accurate view of the convergence of p_ϵ to a Dirac mass in m , and following [8], we introduce a blow-up variable around $m = M$. We set

$$y = \frac{m - M}{\epsilon}, \quad q_\epsilon(\mathbf{x}, \mathbf{v}, y, t) = \epsilon p_\epsilon(\mathbf{x}, \mathbf{v}, m, t) \quad (17)$$

so that

$$\bar{q}_\epsilon(\mathbf{x}, \mathbf{v}, t) := \int_{\mathbb{R}} q_\epsilon(\mathbf{x}, \mathbf{v}, y, t) dy = \int_{\mathbb{R}} p_\epsilon(\mathbf{x}, \mathbf{v}, m, t) dm = \bar{p}_\epsilon(\mathbf{x}, \mathbf{v}, t). \quad (18)$$

Because of these identities, our statements will equivalently be on \bar{q}_ϵ and will go through the analysis of q_ϵ rather than p_ϵ itself.

Also notice that the bounds in (15), (16) also hold true for q_ϵ and \bar{q}_ϵ and allow us to take weak limits.

(i) Without noise. The equation for $q_\epsilon(t, \mathbf{x}, \mathbf{v}, y)$ is written, using the definition in (2),

$$\begin{aligned} \partial_t q_\epsilon + \mathbf{v} \cdot \nabla_{\mathbf{x}} q_\epsilon & - \frac{1}{\epsilon} D_t M \partial_y q_\epsilon + \frac{1}{\epsilon^2} \partial_y (f(\epsilon y) q_\epsilon) \\ & = \int_V \left[\Lambda(y, \mathbf{v}, \mathbf{v}') q_\epsilon(\mathbf{x}, \mathbf{v}', y, t) - \Lambda(y, \mathbf{v}', \mathbf{v}) q_\epsilon(\mathbf{x}, \mathbf{v}, y, t) \right] d\mathbf{v}'. \end{aligned}$$

From (11), we can write $f(\epsilon y) = -\epsilon y G(\epsilon y)$ and the above equation becomes

$$\begin{aligned} \partial_t q_\epsilon + \mathbf{v} \cdot \nabla_{\mathbf{x}} q_\epsilon & - \frac{1}{\epsilon} D_t M \partial_y q_\epsilon - \frac{1}{\epsilon} \partial_y (y G(\epsilon y) q_\epsilon) \\ & = \int_V \left[\Lambda(y, \mathbf{v}, \mathbf{v}') q_\epsilon(\mathbf{x}, \mathbf{v}', y, t) - \Lambda(y, \mathbf{v}', \mathbf{v}) q_\epsilon(\mathbf{x}, \mathbf{v}, y, t) \right] d\mathbf{v}'. \end{aligned} \quad (19)$$

Because q_ϵ is a bounded measure on $\mathbb{R}^d \times V \times \mathbb{R}^+ \times (0, T)$, for all $T > 0$, as $\epsilon \rightarrow 0$, q_ϵ has a weak limit q_0 in the sense of measure (again after extraction) and the above equation gives, in the distributional sense,

$$\partial_y(yG(0)q_0 + D_tM(S)q_0) = 0. \quad (20)$$

From this, we infer that

$$q_0(t, \mathbf{x}, \mathbf{v}, y) = \bar{q}_0(t, \mathbf{x}, \mathbf{v}) \delta\left(y = -\frac{D_tM(S)}{G(0)}\right). \quad (21)$$

This information is useful provided we can establish that

$$\bar{q}_0(\mathbf{x}, \mathbf{v}, t) = \int_{\mathbb{R}} q_0(\mathbf{x}, \mathbf{v}, y, t) dy = \text{weak-}\lim_{\epsilon \rightarrow 0} \bar{q}_\epsilon(\mathbf{x}, \mathbf{v}, t). \quad (22)$$

This step is postponed to Section 4 and involves a control of the tail for large values of m .

We may also integrate equation (19) with respect to y and find in the limit

$$\partial_t \bar{q}_0 + \mathbf{v} \cdot \nabla_{\mathbf{x}} \bar{q}_0 = \int_V \left[\Lambda\left(-\frac{D'_tM}{G(0)}, \mathbf{v}, \mathbf{v}'\right) \bar{q}'_0 d\mathbf{v}' - \Lambda\left(-\frac{D_tM}{G(0)}, \mathbf{v}', \mathbf{v}\right) \bar{q}_0 \right], \quad (23)$$

where $D'_tM(S)$ is the total derivative, as in (2), but in the direction \mathbf{v}' and where \bar{q}'_0 represents $\bar{q}_0(\mathbf{x}, \mathbf{v}', t)$. Finally, for any smooth test function ϕ , we have from the change of variable $m \mapsto y = (m - M)/\epsilon$,

$$\int_{\mathbb{R}} p_\epsilon(\mathbf{x}, \mathbf{v}, m, t) \phi(m) dm = \int_{\mathbb{R}} q_\epsilon(\mathbf{x}, \mathbf{v}, y, t) \phi(M + \epsilon y) dy \rightarrow \bar{q}_0(\mathbf{x}, \mathbf{v}, t) \phi(M),$$

where we use (21). This gives the limiting expression of p_0 in Theorem 2.1.

These are the results stated in Theorem 2.1, if we can establish the relation $\bar{q}_0 = \bar{p}_0$ as stated in (22), which we do later.

(ii) With internal noise. Similarly, after introducing the new variables as in (17), the equation (13) for $q_\epsilon(t, \mathbf{x}, \mathbf{v}, y)$ writes

$$\begin{aligned} \partial_t q_\epsilon + \mathbf{v} \cdot \nabla_{\mathbf{x}} q_\epsilon & - \frac{1}{\epsilon} D_t M \partial_y q_\epsilon + \frac{1}{\epsilon^2} \partial_y (f(\epsilon y) q_\epsilon) \\ & = \frac{\sigma}{\epsilon} \partial_{yy}^2 q_\epsilon + \int_V \left[\Lambda(y, \mathbf{v}, \mathbf{v}') q_\epsilon(\mathbf{x}, \mathbf{v}', y, t) - \Lambda(y, \mathbf{v}', \mathbf{v}) q_\epsilon(\mathbf{x}, \mathbf{v}, y, t) \right] d\mathbf{v}'. \end{aligned}$$

From (11), this equation becomes

$$\begin{aligned} \partial_t q_\epsilon + \mathbf{v} \cdot \nabla_{\mathbf{x}} q_\epsilon & - \frac{1}{\epsilon} D_t M \partial_y q_\epsilon - \frac{1}{\epsilon} \partial_y (yG(\epsilon y) q_\epsilon) \\ & = \frac{\sigma}{\epsilon} \partial_{yy}^2 q_\epsilon + \int_V \left[\Lambda(y, \mathbf{v}, \mathbf{v}') q_\epsilon(\mathbf{x}, \mathbf{v}', y, t) - \Lambda(y, \mathbf{v}', \mathbf{v}) q_\epsilon(\mathbf{x}, \mathbf{v}, y, t) \right] d\mathbf{v}'. \end{aligned} \quad (24)$$

In the limit $\epsilon \rightarrow 0$, the above equation converges to, in the sense of distributions,

$$\partial_y(yG(0)q_0 + D_tMq_0) = -\sigma \partial_{yy}^2 q_0,$$

which shows that

$$q_0(\mathbf{x}, \mathbf{v}, y, t) = \bar{q}_0(\mathbf{x}, \mathbf{v}, t) \sqrt{\frac{G(0)}{2\pi\sigma}} e^{-\frac{G(0)}{2\sigma} \left(y + \frac{D_t M}{G(0)}\right)^2}, \quad (25)$$

a useful information, still assuming we have proved the relation (22) for \bar{q}_0 .

We conclude as before. After integration of (24) with respect to y , passing to the limit $\epsilon \rightarrow 0$, we find

$$\begin{cases} \partial_t \bar{q}_0 + \mathbf{v} \cdot \nabla_{\mathbf{x}} \bar{q}_0 = \int_V \left[T(D'_t M, \mathbf{v}', \mathbf{v}) \bar{q}'_0 - T(D_t M, \mathbf{v}, \mathbf{v}') \bar{q}_0 \right] u d\mathbf{v}', \\ T(D_t M, \mathbf{v}, \mathbf{v}') = \sqrt{\frac{G(0)}{2\pi\sigma}} \int_{\mathbb{R}} \Lambda(y, \mathbf{v}, \mathbf{v}') e^{-\frac{G(0)}{2\sigma} \left(y + \frac{D_t M}{G(0)}\right)^2} dy. \end{cases} \quad (26)$$

The Theorem 2.2 is also proved. \square

4 A priori bounds

We now establish the various estimates which justify that we can pass to the limit as indicated in Section 3 and thus we prove the

Lemma 4.1 *We make the assumptions of Theorem 2.1, then the condition (22) holds and for some constant which depends on $\iint y^2 q^{\text{ini}} dy dx dv$ and $\|M\|_{W^{1,\infty}(\mathbb{R}^d \times \mathbb{R}^+)}$, we have*

$$\iint y^2 q_\epsilon(t) dy dx dv \leq C(q^{\text{ini}}, M).$$

Consequently, q_ϵ converges weakly in the sense of measure towards q_0 and

- (i) for q_ϵ a solution to (19), q_0 is given by (21) with \bar{q}_0 weak solution of (23),
- (ii) for q_ϵ a solution to (24), then, q_0 is given by (25) with \bar{q}_0 weak solution of (26).

Proof. We only consider the case (i) without noise, the case (ii) is obtained by the same token. We first prove some estimates which imply weak convergence. Then, we pass to the limit in the equation satisfied by \bar{q}_ϵ .

L^1 bound. For completeness, we recall that equation (19) is positivity preserving and conservative. It follows the uniform, in ϵ , bound for q_ϵ in L^1 , see (15).

L^∞ bound on \bar{q}_ϵ . We use the notation (18) for \bar{q}_ϵ . Arguing in the spirit of [12, 4, 28]), we first prove the uniform L^∞ bound on \bar{q}_ϵ .

Integrating (19) with respect to y , from the bound (12) and the nonnegativity of q_ϵ , we get

$$\partial_t \bar{q}_\epsilon + \mathbf{v} \cdot \nabla_{\mathbf{x}} \bar{q}_\epsilon \leq \lambda_+ \int \bar{q}_\epsilon d\mathbf{v}'.$$

Then, using the method of characteristics, we have $\partial_t \bar{q}_\epsilon(t, \mathbf{x} + \mathbf{v}t) \leq \lambda_+ \int \bar{q}_\epsilon(\mathbf{x} + \mathbf{v}t, \mathbf{v}', t) d\mathbf{v}'$, which implies after integration

$$\bar{q}_\epsilon(t, \mathbf{x}, \mathbf{v}) - \bar{q}^{\text{ini}}(\mathbf{x} - \mathbf{v}t) \leq \lambda_+ \int_0^t \int \bar{q}_\epsilon(\mathbf{x} - \mathbf{v}s, \mathbf{v}', t-s) d\mathbf{v}' ds.$$

Taking the supremum in \boldsymbol{x} , \boldsymbol{v} , we find

$$\|\bar{q}_\epsilon(t)\|_\infty \leq \|\bar{q}^{\text{ini}}\|_\infty + \lambda_+ |V| \int_0^t \|\bar{q}_\epsilon(s)\|_\infty ds,$$

and using Gronwall's inequality, we find the estimate in (16).

Control on the tail in m . In order to prove the condition (22), we need to ensure that there is no mass loss at infinity in m . To do so, we multiply both sides of (19) by y^2 and integrate by parts with respect to x , v , and y . This yields

$$\frac{d}{dt} \iint y^2 q_\epsilon \, dy \, dx \, dv + \frac{2}{\epsilon} \iint y^2 G(\epsilon y) q_\epsilon \, dy \, dx \, dv + \frac{2}{\epsilon} \iint y D_t M q_\epsilon \, dy \, dx \, dv = 0.$$

Using the Cauchy-Schwarz inequality, we deduce

$$\begin{aligned} \frac{d}{dt} \iint y^2 q_\epsilon \, dy \, dx \, dv + \frac{2}{\epsilon} \iint y^2 G(\epsilon y) q_\epsilon \, dy \, dx \, dv &\leq \frac{1}{\epsilon} \iint y^2 G(\epsilon y) q_\epsilon \, dy \, dx \, dv \\ &+ \frac{1}{\epsilon} \iint (D_t M)^2 \frac{q_\epsilon}{G(\epsilon y)} \, dy \, dx \, dv. \end{aligned}$$

By assumption (10), $D_t M$ is bounded in $L^\infty([0, T] \times \mathbb{R}^d \times V)$. From assumption (11) and the mass conservation, the last integral of the right hand side is uniformly bounded by a constant denoted by $C > 0$. Then from assumption (11), we have,

$$\frac{d}{dt} \iint y^2 q_\epsilon \, dy \, dx \, dv + \frac{g_-}{\epsilon} \iint y^2 q_\epsilon \, dy \, dx \, dv \leq \frac{C}{\epsilon}.$$

From the Gronwall Lemma, we deduce the bound for all $t > 0$,

$$\iint y^2 q_\epsilon(t) \, dy \, dx \, dv \leq e^{-tg_-/\epsilon} \iint y^2 q^{\text{ini}} \, dy \, dx \, dv + \frac{C}{g_-},$$

which implies a uniform bound on $\iint y^2 q_\epsilon(t) \, dy \, dx \, dv$.

Passing to the limit. From the bound above, we deduce that, we can extract a subsequence which converges weakly in measure $q_\epsilon \rightharpoonup q_0$ and such that $\bar{q}_\epsilon \rightharpoonup \bar{q}_0$ in L^∞ -weak*. Then we can pass to the limit in the sense of distribution in equation (19) and deduce that the limit q_0 satisfies equation (20) in the sense of distribution. In fact, we notice that from the Lipschitz character of G , we have

$$\iint y(G(\epsilon y) - G(0)) \bar{q}_\epsilon \, dx \, dy \leq C\epsilon \iint y^2 \bar{q}_\epsilon \, dx \, dy \rightarrow 0, \quad \text{as } \epsilon \rightarrow 0,$$

thanks to the estimate on the tail above. Finally, (20) implies that $yG(0)q_0 + D_t M q_0$ is constant a.e., and this constant should be 0 since from the estimate on the tail above, we have that $yq_0 \in L^1$. We conclude that q_0 vanishes except when $yG(0) + D_t M(S) = 0$. By conservation of the mass, we deduce the expression (21) for p_0 .

5 Comments on physical background

The form of the equation (6) corresponds, for *E. coli* chemotaxis, to the formalism in the physical literature. We have simplified the notations for mathematical clarity and we explain now how to relate our notations to known biophysical quantities. In the presentation below, we have used the same biological parameters as in [14, 26]. Notice that the model below is the most elaborate in terms of biochemistry among the hierarchy in [31].

- The methylation level $M(x, t)$ at equilibrium is related to the extra-cellular attractant profile S , by a logarithmic dependency

$$M = M(S) = m_0 + \frac{f_0(S)}{\alpha}, \quad \text{with} \quad f_0(S) = \ln\left(\frac{1 + S/K_I}{1 + S/K_A}\right).$$

The constant m_0 is a reference methylation level in the absence of signal, the constants K_I and K_A represent the dissociation constants for inactive, respectively active, receptors. Numerical values are given by $\alpha = 1.7$, $m_0 = 1$, $K_I = 18.2\mu M$, $K_A = 3mM$. These parameters were calibrated to fit experimental data [27, 15].

- The receptor activity $a(m, S)$ depends on the intracellular methylation level m and the extracellular chemoattractant concentration S such that

$$a = (1 + \exp(NE))^{-1}, \quad \text{with} \quad E = -\alpha(m - m_0) + f_0(S) = -\alpha(m - M(S)). \quad (27)$$

We note that the specific form of the function a was derived using Boltzmann's law in [29] which can be reduced to the expression (27). The coefficient $N = 6$ represents the number of tightly coupled receptors.

- The intracellular dynamics and tumbling frequency are given by

$$f(m - M(S)) = F(a) = k_R(1 - a/a_0), \quad \Lambda(m - M(S)) = Z(a) = z_0 + \tau^{-1}\left(\frac{a}{a_0}\right)^H,$$

where $a(m, S)$ is the receptor activity defined in (27). The parameter k_R is the methylation rate, a_0 is the receptor preferred activity which is such that $f(a_0) = 0$ and $f'(a_0) < 0$. For the tumbling frequency, z_0 , H , τ represent the rotational diffusion, the Hill coefficient of flagellar motors response curve and the average run time respectively. All these parameters can be measured biologically, their values are given by $k_R = 0.01s^{-1} \sim 0.0005s^{-1}$, $a_0 = 0.5$, $z_0 = 0.14s^{-1}$, $\tau = 0.8s$, $H = 10$.

- Two kinds of noise can be observed in the signaling pathway for *E. coli*, one is from the external fluctuation of the ligand concentration and the other is the internal noise from the random receptor-methylation and demethylation event [7]. For small complexes, the effect on the activity from the external noise is negligible compared to the internal noise.

We refer the readers to [26, 7, 14, 25] and the references therein for the detailed physical meanings of these parameters.

The validity of the assumption $\epsilon \ll 1$ depends on the ratio between $1/k_R$ and the system time. We might have in mind, the time scale of chemotactic signal imposed from outside varies as in the experiments in [26], which motivates the numerical comparisons in section 6. We might also have in mind traveling concentration waves, see [23, 24] and the references in there, where the typical length

is of the order of centimeters, while bacterial velocity is of order of 20 micrometers per second. Then the system time is of the same magnitude as the adaptation time.

Moreover, the Hill coefficient H is large which indicates that $\lambda(m - M(S))$ varies fast with respect to $m - M(S)$. Therefore, the scaling introduced in (6) is satisfied by *E. coli* chemotaxis. We can use

$$f(r) = 1 - \frac{1}{a_0} (1 + \exp(-N\alpha r))^{-1}.$$

Therefore, the function $G(\cdot)$ used in (11) is given by

$$G(r) = -\frac{f(r)}{r} = -\frac{1}{r} \left(1 - \frac{1}{a_0} (1 + \exp(-N\alpha r))^{-1} \right), \quad \text{with } G(0) = -f'(0) = \frac{N\alpha}{4a_0}.$$

Besides, from Theorem 2.1 for the case without noise, using $y = \frac{r}{\epsilon}$ yields

$$\begin{aligned} T(D_t M, \mathbf{v}, \mathbf{v}') &= \Lambda(y, \mathbf{v}, \mathbf{v}') = z_0 + \tau^{-1} \frac{(1 + \exp(-N\alpha \epsilon y))^{-H}}{a_0^H} \\ &= z_0 + \tau^{-1} \frac{(1 + \exp(N\alpha \epsilon D_t M(S)/G(0)))^{-H}}{a_0^H}. \end{aligned}$$

And from Theorem 2.1, when the noise in the methylation level is considered, and choosing $\sigma = 1$,

$$T(D_t M, \mathbf{v}, \mathbf{v}') = \sqrt{\frac{G(0)}{2\pi}} \int_{\mathbb{R}} \Lambda(y, \mathbf{v}, \mathbf{v}') e^{-\frac{G(0)}{2} \left(y + \frac{D_t M}{G(0)} \right)^2} dy.$$

The run durations last longer when bacteria encounter an increasing gradient of chemotactic molecules, this leads to higher bacteria density at the place where the ligand concentration S is higher. This phenomena is well explained by the classical Keller-Segel model which can be considered as the parabolic limit of the kinetic-transport models. However, recent experimental observation shows that higher ligand concentration leading to higher bacteria density is only valid in a spatial-temporal slow-varying environment. When the ligand concentration varies fast, there exists a phase shift between the mass center of ligand concentration and of the bacterias [32]. This is due to the memory effect in the slow methylation adaptation rate. In the limiting kinetic model, $D_t M(S)$ takes into account the memory effect along the trajectory of the moving cell [28]. Then, two interesting questions come: are these two kinds of memory effect the same? Can we see the phase shift between the mass center of ligand concentration and of the bacteria in the limiting kinetic model?

6 Numerical illustrations

We performed numerical simulations using the method SPECS [14]. It is a cell based model that takes into account the evolution of each cell intracellular methylation level, which determines the tumbling frequency of each bacteria. As explained in [25, 26], SPECS and the kinetic model that incorporates intracellular chemo-sensory system (4) show a quantitative match.

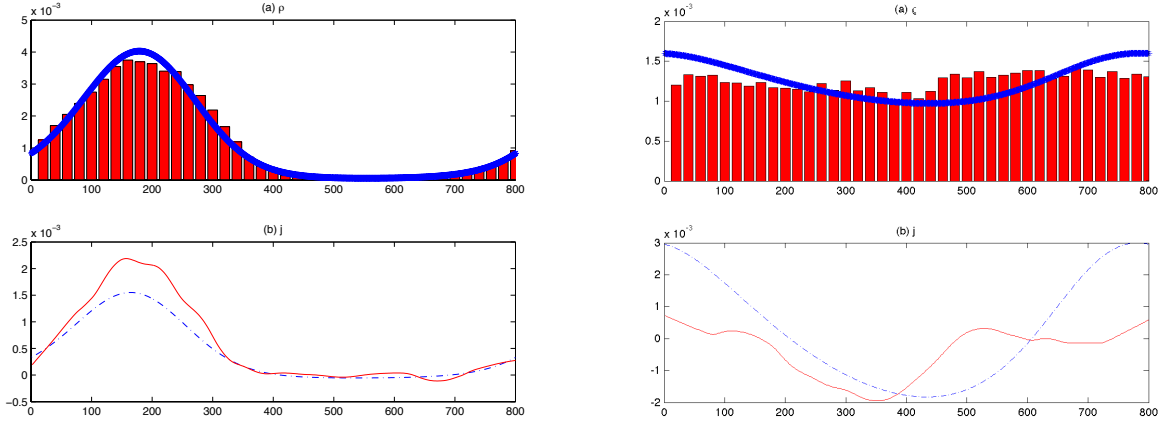


Figure 1: Numerical comparison between the limiting kinetic model and SPECS. The steady state profiles of density ρ (top) and current J (bottom) are presented. Left: $u = 0.4\mu\text{m}/\text{s}$; Right: $u = 8\mu\text{m}/\text{s}$. In the subfigures, histograms and solid lines are from SPECS, while the dash star and dash dotted lines are calculated using the limiting kinetic equation. Parameters used here are $S_0 = 500\mu\text{M}$, $S_A = 100\mu\text{M}$, $\ell = 800\mu\text{m}$. We have used 20,000 cells for simulation with SPECS.

Periodic traveling wave environment:

As in [25, 26], we choose the two velocity kinetic model and a periodic 1D traveling wave concentration

$$S(x, t) = S_0 + S_A \sin\left[\frac{2\pi}{\ell}(x - ut)\right],$$

which is spatial-temporal varying and where the wavelength ℓ is equal to the length of the domain. We compare the numerical results of SPECS and the limiting kinetic model in Figure 1. Upwind scheme is used for the transport terms and periodic boundary conditions are considered. The density is scaled at the order of 10^{-3} , it is the ratio between the actual cell number and the total number. In the Figure 1, the x axis represents the remainder of $x - ut \bmod \ell$, i.e. we keep tracking the wave front of the periodic traveling wave.

Two different wave velocities $u = 0.4\mu\text{m}/\text{s}$ and $u = 8\mu\text{m}/\text{s}$ are considered. We compare the density profiles $\rho = \int_V p \, d\mathbf{v} \, dm$ and the cell flux $J = \int_V \mathbf{v} p \, d\mathbf{v} \, dm$. When the concentrated wave moves slowly, the limiting kinetic model gives good consistency, however in the fast-varying environment, the density and cell flux profiles are different for SPECS and the limiting kinetic model. We refer the readers to [14, 26] for more detailed discussions and physical explanations.

This numerical experiment shows that the memory effect using the model based on $D_t M(S)$ is different from the memory effect for the complete model (4) when fast external chemoattractant waves are considered. This phenomena can be explained by the slow adaptation rate in the methylation level and the memory along the trajectory compared to the phase shift. In this fast wave regime, our mathematical results do not apply because the scaling assumptions are not satisfied.

Exponential Environment

Here we set up an exponential gradient environment $S = S_0 \exp(Gx)$ and numerically compare the average drift velocity of the two different kinetic models. SPECS can be considered as a Monte Carlo simulation for kinetic-methylation model and we constraint ourselves in the space such that

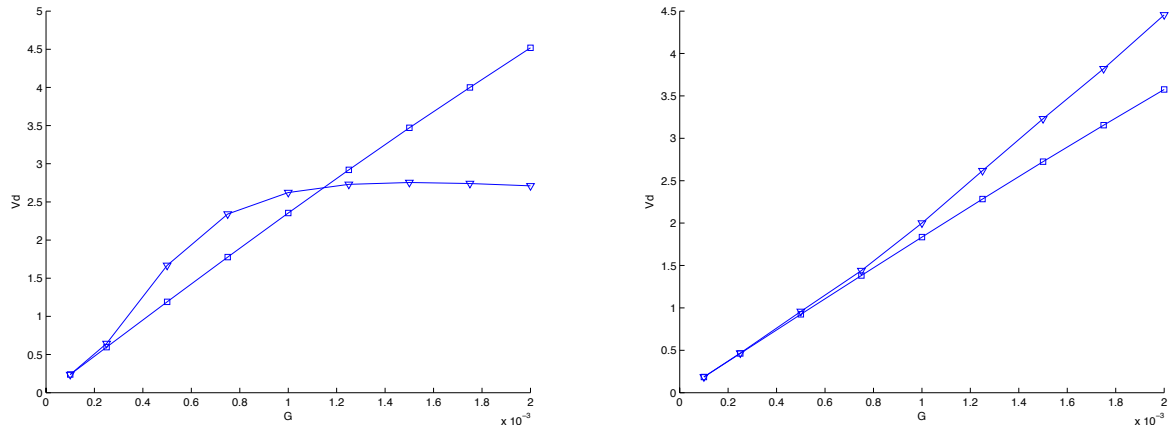


Figure 2: Numerical comparison between the limiting kinetic model and SPECS in the exponential environment. Left: $k_R = 0.005s^{-1}$; right: $k_R = 0.05s^{-1}$. The squares and triangles are respectively for model (1) and (4). The units for G , the abscissae, and the bulk drift velocity V_d , the ordinates, are respectively μm^{-1} and $\mu m/s$. We have used 12,000 cells for simulation with SPECS.

$4K_I < S(x) < K_A/4$. According to [26], when G becomes large and k_R becomes small, the distribution in m is no longer concentrated near $M(S)$, which indicates that the scaling assumption in (6) is violated.

In Figure 2, the average drift velocities of the two kinetic model in the exponential environment for different G and k_R are displayed. When G becomes large, the average drift velocity of the limiting kinetic model is far from what predicted by SPECS. Heuristically, when G increases, the average drift velocity first increases linearly then super-linearly and finally saturate at certain value, the limiting kinetic model can only match the linear regime. Besides, we can observe that larger k_R increases the linearly increasing regime with respect to G .

We compare the distribution of the activity a in Figure 3, a determines the tumbling frequency and it is concentrated as a delta function in the purely kinetic model. We can see that when G is small, the average a for forward and backward moving bacteria in the kinetic methylation model is the same as the concentrated a in the purely kinetic model, while when G becomes large, the average a in the kinetic methylation model is far away from the a in the purely kinetic model. This explains the good match when G is small and the results of the two kinetic model separate when G increase.

7 Discussion

We have shown that the widely used purely kinetic ‘run and tumble’ model (1)–(3) can be derived from a cell based model including the methylation level as internal variables (4)–(5). This link completes the model hierarchy of partial differential equations for bacterial chemotaxis. The derivation of macroscopic model of Keller-Segel type from cell based models or from purely kinetic-transport systems has been widely studied by several authors (see e.g. [8, 5, 9, 16, 6, 30, 23, 11, 13, 25, 31]). Up to our knowledge, this work is the first attempt to link those two latter systems. The derivation is obtained, rigorously, assuming a fast adaptation and a stiff response of the internal variable to the environment changes; it implies the methylation level to be at equilibrium.

For *E. coli* chemotaxis, the smallness assumptions for the derivation is not satisfied. This implies

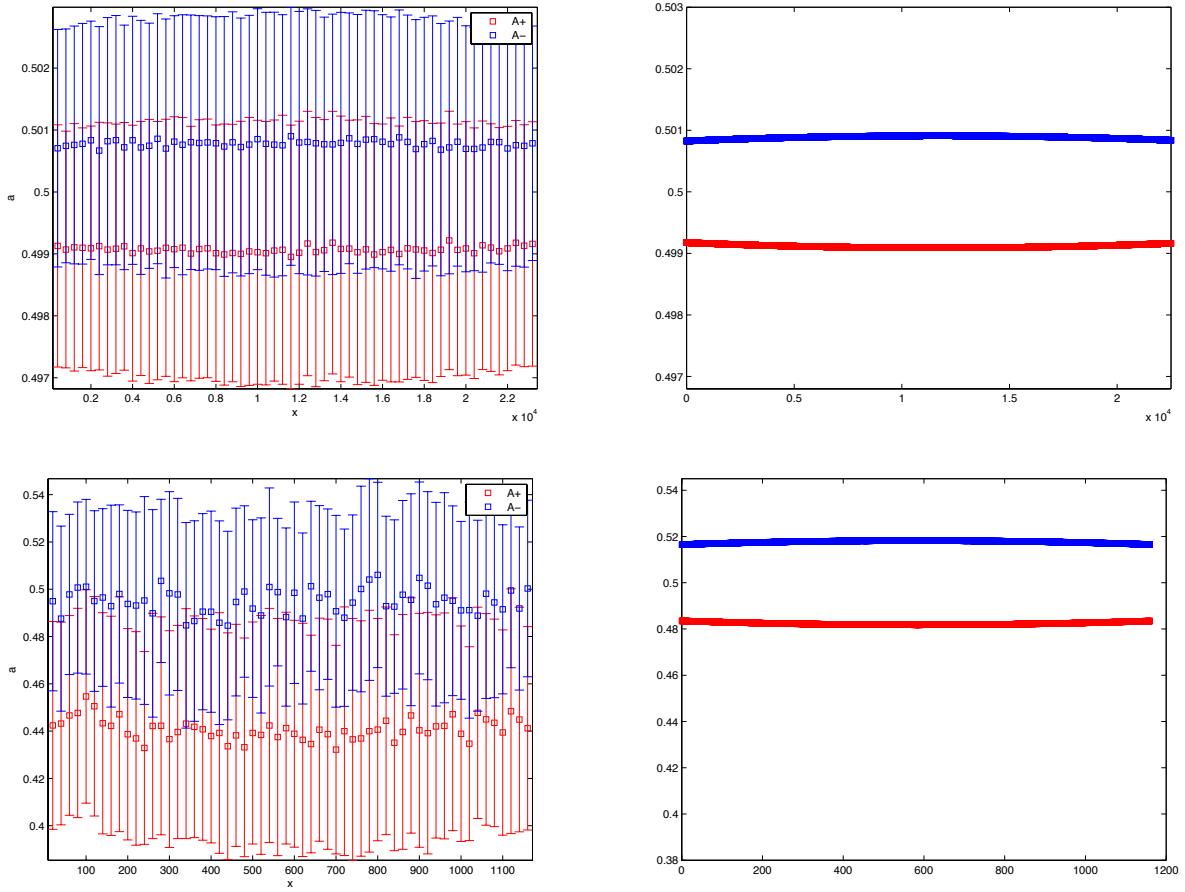


Figure 3: Numerical comparison between the limiting kinetic model and SPECS in the exponential environment. $S_0 = 4K_I = 4 \times 18.2\mu M$. Left: kinetic-methylation model: the mean and variance of the distribution in a for forward (red) and backward (blue) moving bacteria; Right: purely kinetic model: the limiting distribution in a for forward (red) and backward (blue) moving bacteria are delta functions. The top figures are for $G = 0.0001$ while the bottom figures are for $G = 0.002$. Here $k_R = 0.05$.

in particular that for fast varying signals, the kinetic model does not allow to recover the behavior observed thanks to stochastic simulations, see Figure 1-right. We notice that such limitation has been also observed with the Keller-Segel model [31]. Numerical simulations in section 6 show that solutions of the purely kinetic model and the kinetic-methylation model might coincide more broadly than expected with the physical range of parameters chosen for the simulations. A possible explanation might be from the robustness of the limiting procedure as expressed by the Theorem 2.2. However it is possible that a different scaling, still to be discovered, would also produce the purely kinetic limiting equation (1)–(2).

References

- [1] F. Berthelin, N. J. Mauser and F. Poupaud, *high-field limit from a kinetic equation to multidimensional scalar conservation laws*. J. Hyp. Diff. Eq. 4(1) (2007) 123–145.
- [2] N. Bournaveas, V. Calvez, *Critical mass phenomenon for a chemotaxis kinetic model with spherically symmetric initial data* Ann. Inst. H. Poincaré Anal. Non Linéaire 26 (5) (2009), 1871–1895.
- [3] N. Bournaveas, V. Calvez, *Global existence for the kinetic chemotaxis model without pointwise memory effects, and including internal variables*. Kinet. Relat. Models 1 (2008), no. 1, 29–48.
- [4] N. Bournaveas, V. Calvez, S. Gutiérrez, and B. Perthame, *Global existence for a kinetic model of chemotaxis via dispersion and Strichartz estimates*. Comm. P.D.E. 33 (2008), 79–95.
- [5] F. Chalub, P. A. Markowich, B. Perthame, and C. Schmeiser, *Kinetic models for chemotaxis and their drift-diffusion limits*. Monatsh. Math. 142 (2004), 123–141.
- [6] Y. Dolak, C. Schmeiser, *Kinetic models for chemotaxis: Hydrodynamic limits and spatio-temporal mechanisms*. J. Math. Biol. 51 (2005), 595–615.
- [7] R. G. Endres, *Physical principles in sensing and signaling, with an introduction to modeling in biology*, Oxford University Press, 2013.
- [8] R. Erban, H. Othmer, *From individual to collective behaviour in bacterial chemotaxis*. SIAM J. Appl. Math. 65(2) (2004), 361–391.
- [9] R. Erban, H. Othmer, *Taxis equations for amoeboid cells*. J. Math. Biol. (2007) 54:847–885.
- [10] G. L. Hazelbauer, *Bacterial chemotaxis: the early years of molecular studies*. Annu Rev Microbiol (2012) 66:285–303.
- [11] T. Hillen and K. Painter, *Transport and anisotropic diffusion models for movement in oriented habitats*. Dispersal, Individual Movement and Spatial Ecology: A mathematical perspective. Eds: M.A. Lewis, P. Maini, S. Petrowskii, Heidelberg, Springer, 2012, 177–222.
- [12] H. J. Hwang, K. Kang, A. Stevens, *Global Solutions of Nonlinear Transport Equations for Chemotaxis*. SIAM. J. Math. Anal. 36 (2005) 1177–1199.
- [13] F. James, N. Vauchelet, *Chemotaxis : from kinetic equations to aggregate dynamics*. Nonlinear Diff. Eq. Appl. 20(1), (2013), 101–127.

- [14] L. Jiang, Q. Ouyang, and Y. Tu, *Quantitative modeling of Escherichia coli chemotactic motion in environments varying in space and time*. PLoS Comput. Biol. 6 (2010), e1000735.
- [15] Y. V. Kalinin, L. Jiang, Y. Tu, and M. Wu, *Logarithmic sensing in Escherichia coli bacterial chemotaxis*. Biophys. J. (2009) 96(6):2439–2448.
- [16] J. T. Locsei, *Persistence of direction increases the drift velocity of run and tumble chemotaxis*. J. Math. Biol. 55 (2007), no. 1, 41–60.
- [17] J. Liao, *Global solution for a kinetic chemotaxis model with internal dynamics and its fast adaptation limit*. J. Diff. Eq. (2015), 259 (11), 6432–6458.
- [18] H. Othmer, S. Dunbar, and W. Alt, *Models of dispersal in biological systems*. J. Math. Biol., 26 (1988), 263–298.
- [19] H. G. Othmer, and T. Hillen, *The diffusion limit of transport equations II: Chemotaxis equations*. SIAM J. Appl. Math., 62 (2002), 122–1250.
- [20] H. G. Othmer, X. Xin, and C. Xue, *Excitation and adaptation in bacteria—a model signal transduction system that controls taxis and spatial pattern formation*. Int J Mol Sci (2013) 14(5):9205–9248.
- [21] S. L. Porter, G. H. Wadhams, and J. P. Armitage, *Rhodobacter sphaeroides: complexity in chemotactic signalling*. Trends Microbiol (2008) 16(6):251–260.
- [22] C. V. Rao, J. R. Kirby, and A. P. Arkin, *Design and diversity in bacterial chemotaxis: a comparative study in Escherichia coli and Bacillus subtilis*. PLoS Biol (2004) 2(2):E49.
- [23] J. Saragosti, V. Calvez, N. Bournaveas, A. Buguin, P. Silberzan, and B. Perthame. *Mathematical description of bacterial traveling pulses*. PLoS Comput Biol, 6(8) :e1000890 (2010). doi:10.1371/journal.pcbi.1000890
- [24] J. Saragosti, V. Calvez, N. Bournaveas, B. Perthame, A. Buguin, and P. Silberzan. *Directional persistence of chemotactic bacteria in a traveling concentration wave*. Proceedings of the National Academy of Sciences, 108(39) (2011), 16235–16240.
- [25] G. Si, M. Tang, and X. Yang, *A pathway-based mean-field model for E. coli chemotaxis: mathematical derivation and keller-segel limit*. Multiscale Model Simul. 12(2), (2014), 907–926.
- [26] G. Si, T. Wu, Q. Ouyang, and Y. Tu, *A pathway-based mean-field model for Escherichia coli chemotaxis*. Phys. Rev. Lett. 109 (2012), 048101.
- [27] Y. Tu, T.S. Shimizu, and H.C. Berg, *Modeling the chemotactic response of Escherichia coli to time-varying stimuli*. Proc Natl Acad Sci USA (2008) 105(39): 14855–14860.
- [28] N. Vauchelet, *Numerical simulation of a kinetic model for chemotaxis*. Kin. Rel. Models., Vol 3, no 3 (2010), 501–528.
- [29] X. Xin, and H. G. Othmer, *A trimer of dimers-based model for the chemotactic signal transduction network in bacterial chemotaxis*. Bull Math Biol (2012) 74(10):2339–2382.
- [30] C. Xue, and H. G. Othmer. *Multiscale models of taxis-driven patterning in bacterial populations*. SIAM J. Appl. Math., Vol. 70, no. 1,(2009), 133–167.

- [31] C. Xue *Macroscopic equations for bacterial chemotaxis: integration of detailed biochemistry of cell signaling*. J. Math. Biol. Vol. 70, (2015), 1–44.
- [32] X. Zhu, G. Si, N. Deng, Q. Ouyang, T. Wu, Z. He, L. Jiang, C. Luo, and Y. Tu, *Frequency-dependent Escherichia coli chemotaxis behavior*. Phys. Rev. Lett., 108 (2012), 128101.